Thermal Solar Collector Behaviour in Romania

Mugur C. Bălan[1]*, Lorentz Jäntschi[1]**, Sorana Bolboacă[2]***, Mihai Damian[1]****

[1]Technical University of Cluj Napoca, 103-105 Muncii Bvd, 400641 Cluj-Napoca, Romania
[2]"Iuliu Hațieganu" University of Medicine and Pharmacy Cluj-Napoca, 13 Emil Isac, 400023 Cluj-Napoca, Romania

Abstract

Our study of thermal solar collectors' behaviour in a transitory regime covered a period of 9 months, from August 2007 to May 2008. The data were measured using two pyranometers (one shaded) and were recorded into a database with a baud rate of 50 seconds. Sun a position was calculated using a previously reported mathematical model embedded into an online software application. Standard technical parameters of solar thermal collectors were used to estimate their efficiency at the measuring location.

Results reflect the particular conditions at Cluj-Napoca, Romania, and provide a local solar energy potential evaluation. Influences of a collector's type and time of year on thermal solar collectors' efficiency, thermal power, and accumulated heat are given. The described methodology and procedure of assessment are general and may be applied anywhere.

Keywords: embedded systems, solar radiation measurements, solar collectors, solar heating efficiency

Introduction

In order to design performing solar water heating systems in the most efficient possible way, a detailed analysis of all the components must be realized. In this analysis, the thermal solar collectors will always be of major importance.

A series of studies shows the high interest for the development of new solar collectors [1], for modelling of the behaviour of existing solar systems [2, 3], for testing [4, 5], and use [6]. Modelling of the solar radiation [7] and predictions of the solar thermal collector's behaviour [8] must be also considered, taking into account the key applications in different fields [9].

As long as both technical and economical elements are involved, cheaper but less efficient solar collectors and expensive but more efficient collectors must be equally considered. Some studies suggest that cheaper and simpler solar collectors, like the unglazed ones, have great economic advantages [10] but other type of collectors are much more efficient.

The types of thermal solar collectors analyzed in the paper are designed to be integrated in different domestic thermal systems such as water or swimming pool heating. In the process of thermal solar collector sizing, the heating demand must be calculated, (this activity can be done as indicated in [11]).

Behaviour and efficiency is analyzed for the following types of thermal solar collectors: *unglazed collectors* (unglazed), *flat collectors* (flat), *evacuated tube collectors* (evacuated) and *evacuated tubes with heat pipe collectors* (heat pipes). Due to the relatively similar range of performances, the evacuated and heat pipe collectors were treated together as evacuated collectors.

This study follows the continuous monitoring process of solar radiation over nine months starting in August 2007. Some preliminary results of the monitoring process were presented in [12]. In order to estimate the efficiency of the thermal solar collectors, some mathematical models concerning solar radiation were implemented and used [13, 14].

*e-mail: mugur.balan@termo.utcluj.ro
**e-mail: lori@academicdirect.ro
***e-mail: sbolboaca@umfcluj.ro
****e-mail: mihai.damian@tcm.utcluj.ro

Table 1. Typical values of optical efficiency and correction factors for different collectors.

Type	Model	η_0 [%]	k_1 [Wm⁻²K⁻¹]	k_2 [Wm⁻²K⁻²]
Unglazed	Energie Solaire	94.80	12.28	0.0235
Flat	Winkler VarioSol A-antireflex	82.50	3.13	0.0152
Flat	Rehau Solect Fassadenkollektor	78.50	3.66	0.0070
Flat	Arge Integral Holz	77.70	4.36	0.0101
Evacuated	Riomay Ecotube	79.40	1.02	0.0032
Evacuated	Enertech EnerSol HP	73.90	1.08	0.0056
Evacuated	Spring Solar SK-8 CPC	62.00	0.94	0.0070
Heat pipes	Thermomax Mazdon 20	76.00	1.09	0.0061
Heat pipes	Dallinger Sonnenpower 22	61.70	1.34	0.0101
Heat pipes	Kilimeko KS 1800/58-18	53.30	1.30	0.0125

Type: collector type; Model: collector model; η_0: optical efficiency; k_1, k_2: correction factors adapted from Solartechnik Prüfung Forschung of Switzerland: http://www.spf.ch/spf.php?lang=en&fam=1&tab=1 – May 2009.

By using the data regarding direct and diffuse radiation recorded in our location, theoretical and practical considerations about the thermal solar collector's behaviour in a transitory working regime were drawn. A software application was developed to perform all the calculations.

Material and Method

Looking for parameters of all types of solar collectors, the standard ones can be found from a manufacturer or at independent testing laboratories. A fair approach was considered to use data provided by one independent testing laboratory.

For the study, we analyzed data from Solartechnik Prüfung Forschung of Swiss (SPF-CH) (http://www.spf.ch/spf.php?lang=en&fam=1&tab=1).

A mathematical equation for calculating solar thermal efficiency, recommended in [15] and [16] (as in many manuals and web sites), can be applied to all types of thermal solar collectors, including evacuated tube collectors or heat pipes collectors:

$$\eta = \eta_0 - k_1 \frac{\Delta t}{I_{gt}} - k_2 \frac{\Delta t^2}{I_{gt}} \qquad (1)$$

...where: η_0 is optical efficiency; k_1 [Wm⁻²K⁻¹] and k_2 [Wm⁻²K⁻²] are correction factors and characteristics for thermal losses; Δt is the difference between the average temperature of the thermal agent and the ambient temperature; I_{gt} [W·m⁻²] is the global radiation intensity, normal at the collector surface.

Factors k_1 and k_2 are dependent on collector construction and are reported to the aperture area (the surface through which the non-concentrated solar radiation enters into the collector). The values of optical efficiency and of the correction factors k_1 and k_2, for some models of solar collectors are presented in Table 1.

Analysis of the values from Table 1 revealed that even if the unglazed and flat collectors have a high value of the optical efficiency, they also have high values for thermal losses.

It must be equally observed that in equation (1) global solar radiation, normal at the collector's surface, must be used. In the transitory working regime of the thermal solar collectors, both solar radiation and temperature difference are continuously modifying. This variability appears because the solar radiation and the angle between the normal at the collector's surface and the direction of the Sun are variable. The orientation angles of the collectors are also representing important parameters of the whole system. In the frame of this study, it was considered that the collectors are oriented through the South and tilted from the horizontal at 45°.

The online solar radiation monitoring system developed at the Technical University of Cluj-Napoca (TUCN), Romania, and described in [12], measure both global and the diffuse radiation in a horizontal plane. Direct radiation in the same horizontal plane is equally calculated and provided. The presented results correspond to the location of the online solar radiation monitoring system: *latitude* φ = 46°47.758' N and *longitude* λ = 23°37.563' E.

In order to compute the value of the normal global radiation to the tilted surface of the solar collector, the mathematical model presented in [16] was implemented in order to calculate the position of the Sun on the sky.

As follows, details of the mathematical model implementation are given.

The Sun's position depends on the location of the observer. Thus, the software application that was developed becomes able to perform calculations for any location indicated by the two coordinates, *latitude* (φ) and *longitude* (λ). The parameters involved in the mathematical model are:

- Day angle (y; [°]): ratio between the day of the year and the number of the days of the year; y = 360°·(day of the year / number of the days of the year).
- Declination of the Sun (δ; [°]): angle between the rays of the sun and the plane of the Earth's equator; δ varies during the year. The maximum value of the declination is δ = 23°27' at the solstices (δ = +23°27' at the northern hemisphere summer solstice and δ=-23°27' at the northern hemisphere winter solstice). The minimum value of the declination is δ is 0° at the equinoxes; δ(y) = 0.3948 - 23.25559·cos(y + 9.1°) - 0.3915·cos(2y + 5.4°) - 0.1764·cos(3y + 105.2°).
- The equation of time (EQT; [min]): the difference over the course of a year between the time as read from a sundial and a clock; EQT (y) = 0.0066 + 7.3525·cos(y + 85.9°) + 9.9359·cos(2y + 108.9°) + 0.3387·cos(3y + 105.2°).
- Mean local time (MLT; [min]): depends on local time (LT), time zone (TZ) and longitude (λ) of the location (here LT-TZ=EET; EET - Eastern European Time shift); MLT = LT - TZ + λ·4 min/°.
- Solar time (ST; [h]): hour angle of the Sun (angle expressed in time units); ST = MLT + EQT.
- Hour angle of the Sun (ω; [°]): angle between the half plane determined by the Earth axis and the zenith and the half plane determined by the Earth axis and the direction of the Sun; ω = (12 - ST)·15°/h.
- The angle of the solar altitude (γ$_S$; [°]) and the angle of solar azimuth (α$_S$; [°]): indicate the position of the Sun relative to an observer on the Earth's surface (Fig. 1); γ$_S$ = arcsin(cos(ω)·cos(φ)·cos(δ) + sin(φ)·sin(δ)); α$_S$ = 180° ± arcos((sin(γ$_S$)·sin(φ) - sin(δ))/(cos(γ$_S$)·cos(φ))); ± = "+" if ST > 12:00 and "-" if ST < 12:00.
- Solar angle of incidence on a tilted surface (θ; [°]): angle between the normal direction at the tilted surface (collector) and the direction of the Sun (Fig. 1); θ = arcos (- cos(γ$_S$)·sin(γt)·cos(α$_S$ - α$_t$) + sin(γ$_S$)·cos(γ$_t$)).
- Global solar radiation on a tilted surface (I$_{gt}$; [Wm^{-2}]) has three components: direct normal radiation on a tilted surface (I$_{dirt}$), diffuse normal radiation on a tilted surface (I$_{dift}$), and ground-reflected normal radiation on a tilted surface (I$_{grt}$); I$_{gt}$ = I$_{dirt}$ + I$_{dift}$ + I$_{grt}$.

- Reflected normal radiation on a tilted surface (I$_{grt}$) - can be calculated as: I$_{grt}$ = I$_{gt}$·A·(1 - cos(γ$_t$)), where A represents the extent to which the horizontal surface diffusely reflects the solar radiation (Albedo). The flat collectors are insulated on the back side, where the reflected radiation is influencing the collector. The evacuated and heat pipes collectors, they are usually coated with selective materials that don't absorb the wavelength of the infrared ground-reflected radiation. In these conditions, in the case of thermal solar collectors, the ground-reflected radiation does not contribute to the useful heating effect and reflected radiation could be neglected in the study.
- Direct normal radiation on a tilted surface (I$_{dirt}$): can be calculated as: I$_{dirt}$ = I$_{dir}$·cos(θ)/sin(γ$_S$), where I$_{dir}$ represents direct solar radiation on a horizontal surface: measured by the solar radiation monitoring system.
- Diffuse normal radiation on a tilted surface (I$_{dift}$): can be calculated considering the diffuse radiation constant across the whole sky (isotropic assumption, I$_{difti}$), indicated in [16, 17]), or considering diffuse radiation with different values on different directions (anisotropic assumption, I$_{difta}$) indicated in [16, 18]): I$_{difti}$ = I$_{dif}$·(1 + cos(γ$_t$))/2; I$_{difta}$ = I$_{dif}$·(1 + F + sin^3(γ$_t$/2))·(1 + F + cos^2(θ)·cos^3(γ$_S$)), where I$_{dif}$ represents the diffuse solar radiation on a horizontal surface measured by a solar radiation monitoring system, and factor F can be calculated as: F = 1 - (I$_{dir}$/I$_g$)^2, where I$_g$ represents the global radiation on a horizontal surface, measured by the solar radiation monitoring system.

The presented mathematical model was implemented into an online software application and used together with solar radiation measurements in order to highlight relevant aspects of a thermal solar collector's behaviour in Cluj-Napoca, Romania [url: http://l.academicdirect.org/Engineering/environment/heat].

Results and Discussion

To highlight the conditions in which all graphical representations were drawn, the following abbreviations were
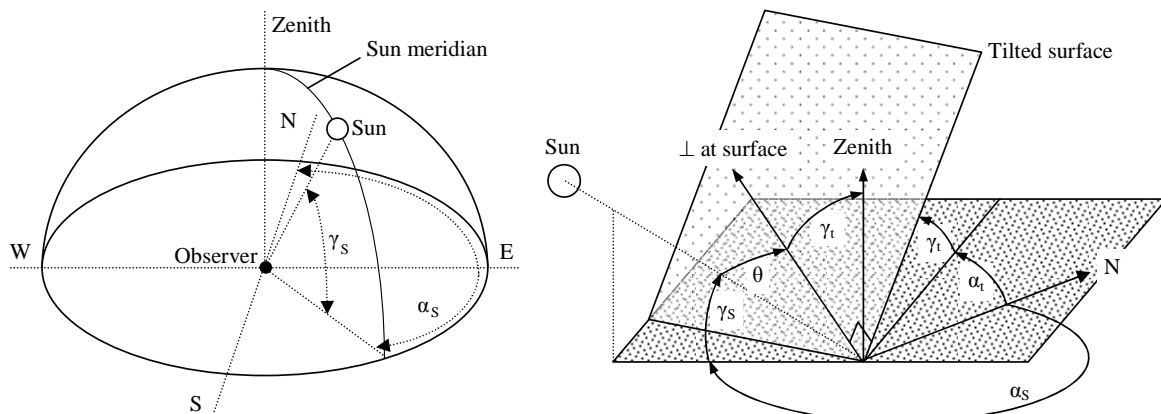

Fig. 1. Solar altitude (γ$_S$), solar azimuth (α$_S$), and solar angle of incidence on a tilted surface (θ).

Table 2. Real and computed sun declination values.

Values	Day	2007.08	2007.09	2007.10	2007.11	2007.12	2008.01	2008.02	2008.03	2008.04	2008.05
Computed	21	+12°27'	+1°09'	-10°35'	-19°57'	**-23°17'**	-19°53'	-10°59'	**0°06'**	+11°59'	+20°21'
	22	+12°08'	+0°45'	-10°57'	-20°10'	**-23°17'**	-19°41'	-10°38'	+0°30'	+12°20'	+20°32'
	23	+11°48'	**+0°21'**	-11°19'	-20°23'	**-23°16'**	-19°28'	-10°17'	+0°54'	+12°40'	+20°44'
Observed	21	+12°19'	+0°57'	-10°29'	-19°47'	**-23°26'**	-20°05'	-10°52'	**0°00'**	+11°39'	+20°04'
	22	+11°59'	+0°33'	-10°50'	-20°00'	**-23°26'**	-19°52'	-10°30'	+0°24'	+12°00'	+20°16'
	23	+11°39'	**+0°10'**	-11°12'	-20°13'	**-23°26'**	-19°38'	-10°08'	+0°47'	+12°20'	+20°28'

Computed: using mathematical model described above
Observed: from www.wsanford.com/~wsanford/exo/sundials/DEC_Sun.html – May 2009.

used at the end of each figure caption; abbreviations concerning the manner in which the results were obtained (first letter) and concerning the surface for which the results were calculated or measured (second letter):
- *E*: Results obtained from experimental measurements (experimental results);
- *T*: Results obtained from a mathematical model (theoretical results);
- *A*: Results representing theoretical averages (of local outside temperature);
- *M*: Results obtained from a combination of experimental measurements and theoretical estimations;
- *H*: Results obtained for horizontal plane/surface;
- *T*: Results obtained for tilted plane/surface.

On some graphical representations we used combinations of the two categories of abbreviations (e.g.: *EH* – experimental results obtained for the horizontal surface; *MT* – results obtained from a combination of experimental measurements and theoretical estimations for a tilted surface, etc.).

All the results, theoretical and experimental, were obtained at the location of the solar radiation monitoring system. In order to validate the implementation of the mathematical model, for the computation of the Sun position on the sky, the obtained results were carefully compared, with known values of astronomical data concerning the sun's position and by correlating some of the simulation results with the measured solar radiation.

The real and computed values of sun declination, for the months in which the solar radiation monitoring system was operational, are presented in Table 2. The observed values are the mean values for the four years of a leap-year cycle [www.wsanford.com/~wsanford/exo/sundials/DEC_Sun.html].

The bold values correspond to the equinoxes and solstice. It can be observed, that the errors between the real average values and the calculated values are in all the considered days of the year, lower than 20' equivalent with 0.3°. Between observed and computed values of sun declination, presented in Table 2, the strength of the linear relationship was assessed using a series of correlation coefficients. Three types of measurements (correlation coefficients) were involved [21]: quantitative (Pearson r) as a measure of the

relationship between values, qualitative (Spearman ρ, Kendall's τ_a, τ_b, and τ_c and Goodman-Kruskal Γ) as measurements of the relationship between ranks (with or without ties influence), and semi-quantitative (as geometrical mean of Pearson and Spearman correlation coefficients). The weakest linear relationships were achieved when Kendall τ_c measures the qualitative association ($\tau_c = 0.9444$; $\tau_c^2 \approx 89\%$; probability to observe a better association: $p = 2.3 \cdot 10^{-13}$), and the strongest one when Pearson r measures the quantitative association ($r = 0.9999$; $p = 1.8 \cdot 10^{-58}$).

The analysis of statistical results leads to the conclusion that from all the different points of view, the calculated values are in strong agreement with the observed ones, giving enough confidence (over 89%) on the values provided by the implemented mathematical model. Fig. 2 presents a solar position diagram, traced for five days in different months with solar radiation monitoring in 2007 (the same days as in Table 2).

The solar azimuth angle (Fig. 2) represents the cardinal directions: N=0°; E=90°; S=180° and W=270°.

It can be observed that on the day corresponding to the equinox 2007.09.23, the simulated position diagrams indicate that sunrise and sunset positions are exactly corresponding to the east and west. For the same period we used values recorded by the online solar radiation monitoring system for global radiation (Fig. 3).

The analysis of Fig. 3 revealed that for the two day of equinox, the measured global radiation started to grow exactly when the simulated position of the Sun correspond-
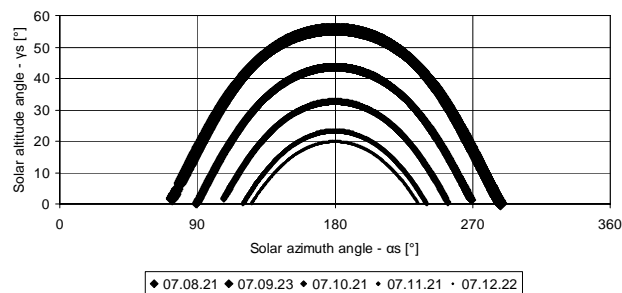

Fig. 2. Solar position diagram for five days in different months of 2007 – *T*.

ed to the east (solar azimuth angle of 90°). In the same way the values of the measured global radiation became equal to zero, exactly when the simulated position of the sun is corresponding to the west (solar azimuth angle of 270°). For the rest of the considered days, it can be observed that the values of the measured global radiation are positive exactly in the period of time between the simulated sunrise and sunset. Equally, it can be observed that the positions of the simulated sunrise and sunset correspond to the positions where the measured global solar radiation is starting to grow over zero (sunrise), or is starting to be zero (sunset).

These elements are convergent to the conclusion that the mathematical model used to calculate the position of the sun on the sky, less for the location of the online solar radiation monitoring system, is correct and was correctly
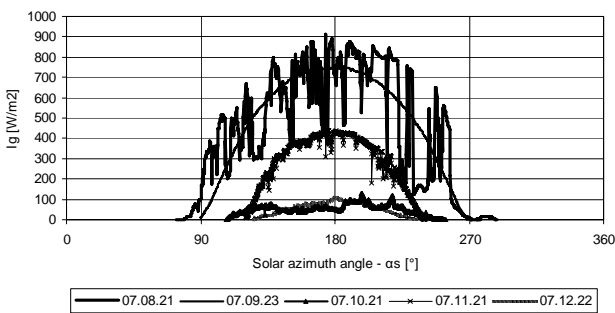
implemented into the developed client-server application software. Unreasonable values were obtained only for the calculated values of direct and diffuse radiation normal on the tilted collector's surface, and only for very low values of the solar altitude angle (γ_S). This limit of the mathematical model was known [15, 16]. In order to eliminate from the results these undesirable situations, the calculations were performed only for values of the solar altitude angle (γ_S) higher than 7°.

Fig. 4 presents the solar angle of incidence variation during the year for different days of the year, considering the surface tilted with 45° from the horizontal plane and oriented exactly south. The value of this angle is very important for calculations influencing both direct radiation and anisotropic diffuse radiation on the tilted surface of the collector.

In order to study the behaviour of different thermal solar collectors in a transitory regime, we chose four different months of the period August 2007-May 2008, different days (one for each month), for which the measured values of the global solar radiation indicated that the sky was clear (or almost clear) for each. The online solar radiation monitoring system developed at the TUCN was used in this task. The results of comparison between our measurements and those provided by the local meteorological station showed that there are no significant differences between the two measurements [12]. In these conditions, it was possible to continue and to extend our studies concerning the available solar radiation in Cluj-Napoca. Recorded global solar radiation on a horizontal surface (I_g, [Wm^{-2}]) (at solar altitude angle (γ_S) higher than 7°) for the days in 2007 (08.17; 10.17; 01.30) and 2008 (03.28 and 05.06) are given in Fig. 5. Global solar radiation, normal at the collector's surface, (45° tilted from horizontal, oriented through south, calculated with data from both Figs. 4 and 5) is given in Fig. 6.

By comparing Figs. 5 and 6, we can observe on a tilted thermal solar collector surface that a higher value of incident solar radiation (normal at the collector surface) will be available for the whole year. The values of the solar radiation on the tilted surface are increasing in different manners, for different periods of the year:
- Lower for the days with high solar radiation on horizontal surface (see 2008.05.06);
- Higher for the days with low solar radiation on horizontal surface (see 2008.01.30).

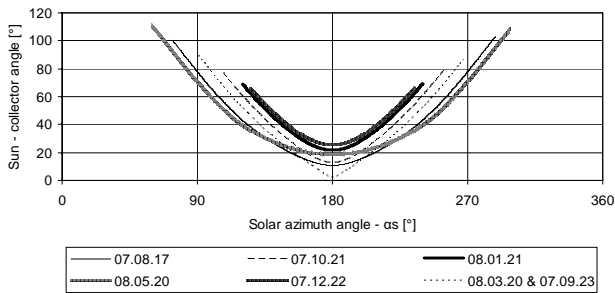Fig. 3. Recorded global radiation, for five days in different months of 2007 – **E**.

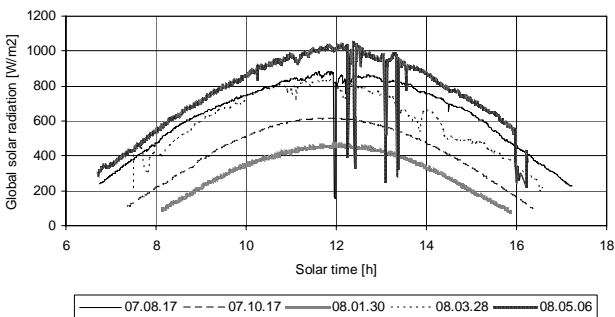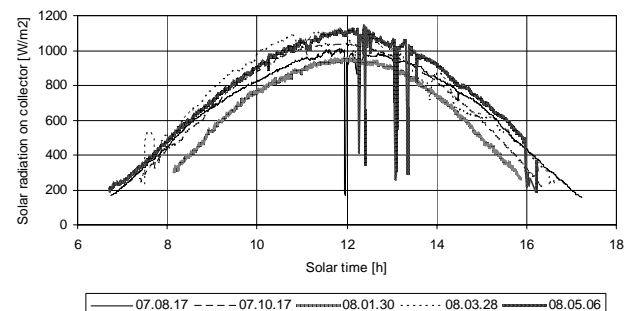Fig. 4. Variation of the Solar angle of incidence on a 45° tilted surface – **T**.

Fig. 5. Recorded values of global solar radiation on horizontal surface – **EH**.

Fig. 6. Global solar radiation on a surface tilted at 45° from horizontal and oriented through the south – **MT**.

Table 3. Average temperatures, daily amplitude and moment of maximum temperature in Cluj-Napoca.

Month	Aug.	Oct.	Jan.	Mar.	May
Temperature [°C]	18	9	-3	4	14
Amplitude [°C]	7	5	3	4	5
Max. moment [hh:mm]	14:30	13:30	12:00	13:00	14:00

from http://www.weatherbase.com/weather/weatherall.php3?s=2151&refer=&units=metric – May 2009.

The benefit of tilting the collector surface is not uniform during the whole periods with the sun on the sky. The higher advantages will be reached around the middle of the days and lower advantages will be reached during the periods in the vicinity of sunrise and sunset.

The monitoring system, designed for solar radiation only, did not record the ambient temperature variation, which must also be known in order to determine the collector's efficiency. It was assumed that in the considered days, with clear or almost clear sky, from the month for which it was drawn, the solar radiation variation curve, the temperature variation was sinusoidal around the average temperatures during the years in each month. The average temperatures and the amplitude of the sinusoidal daily temperature variation, for Cluj-Napoca (available in different meteorological databases) are presented in Table 3.

With these assumptions, the daily temperature variation was determined for each month of the year and these temperature variations were considered as being similar during all the days of each month.

Fig. 7 presents the outside temperatures in the same previously considered days of the year, for solar altitude angles (γ_S) higher than 7°.

The instantaneous temperature difference was calculated as the difference between the average temperature of the thermal agent inside the solar collectors and the outside temperature.

The working thermal regime of the solar collectors was assumed to be constant (which is not really accurate). The average temperature of the thermal agent inside the collectors was considered to be 65°C. (Of course in the real working regime of the solar collectors variations from this value will be met).
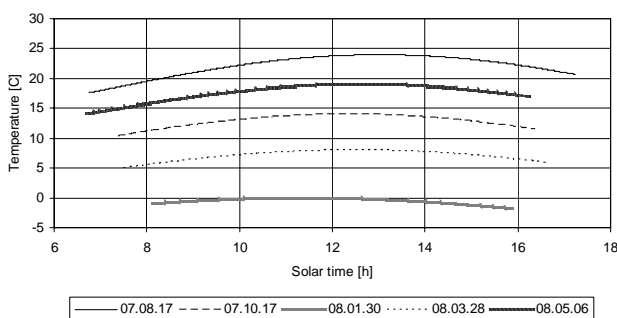

Fig. 7. Assumed daily temperature variation in different days of the year – *A*.

Even with these assumptions, the mathematical model to calculate the solar collector's efficiency remains sufficiently accurate for technical applications, but the results must be considered relevant only for the trend of the thermal solar collector efficiency variation, characteristic for the transitory working regime of these collectors.

The data recorded by the solar radiation monitoring system, available at the Technical University of Cluj-Napoca, allow the calculation of the continuous variation of the solar collector's efficiency, but this paper presents only values for the mentioned representatives on a clear or almost clear sky during considered days.

In order to evaluate the behaviour of the thermal solar collectors, in the developed software application we used the optical efficiency and correction factors for 160 solar collectors of the following types: unglazed, flat, evacuated, and heat pipes.

The three parameters provided by the independent testing laboratory SPF-CH or by some solar collector providers (optical efficiency and correction factors) were used to simulate the behaviour of the solar collectors.

In order to provide significant results with a wide range of availability, we chose collectors with high and low performances for each of the following types: flat, evacuated, and heat pipes. The results obtained for the single available unglazed collector were equally provided.

The behaviour of the thermal solar collectors was characterized by three parameters: thermal efficiency (η, [-]), thermal power (P, [Wm^{-2}]), and heat accumulated in the thermal agent (Q, [MJm^{-2}]).

Thermal power (P) was calculated as a product between global solar radiation on the tilted surface of the collector (I_{gt}) and thermal efficiency (η).

The component of the accumulated heat from the diffuse radiation was calculated both as isotropic and as anisotropic. Since (as indicated in [18]) the anisotropic model is more accurate, it presented only the accumulated heat obtained with the diffuse component of the solar radiation, considered to be anisotropic. The heat accumulated in the thermal agent was calculated as the product between the thermal power and the operating time.

Figs. 8 and 9 give thermal efficiency and thermal power for the unglazed collector in different days.

The higher values of the thermal efficiency for the unglazed collector, for the considered days of August and May, were about 45%, but the higher value of the same parameter in January was about 10%. In the days of October and March, the higher values of thermal efficiency were about 30-35%.

It must be noticed that the higher efficiency of this collector type can be reached only for short periods of time.

The higher values of the thermal power for the unglazed collector in the considered days were about 500Wm^{-2} in May, about 400Wm^{-2} in August and about only 100Wm^{-2} in January. The higher values of thermal power in May compared to August, in the conditions of almost similar values of the thermal efficiency, can be explained by the higher values of global solar radiation on the tilted surface of the collector, in May compared to August. In winter, this type of
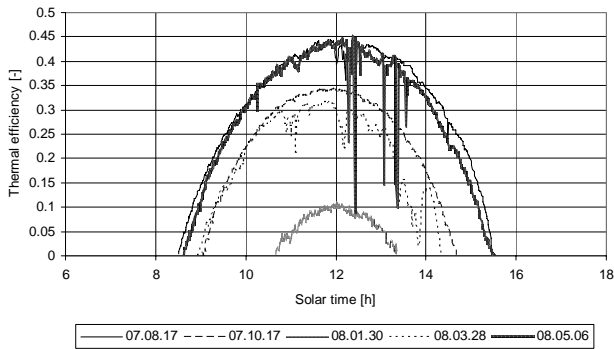
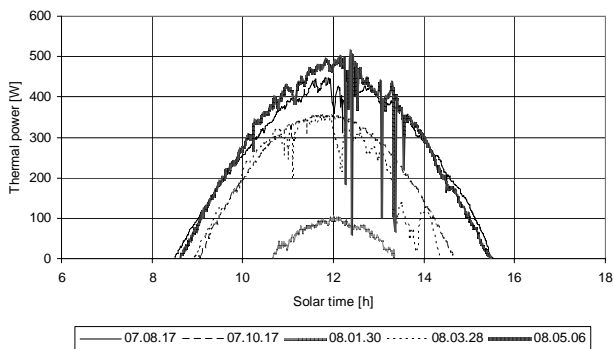Fig. 8. Thermal efficiency for unglazed collector – **MT**.

Fig. 9. Thermal power for unglazed collector – **MT.**

collector is practically not efficient at all, because the maximum value of the thermal power was of only 100Wm^{-2} and in many others less sunny days, this value is decreasing at 0 Wm^{-2}.

Figs. 10 and 11 give thermal efficiency and thermal power for a high performance flat collector in different days.

The higher values of thermal efficiency for the high-performance flat collector (for the days of August and May, but also October and March) were about 65-70%. The higher value of the same parameter in January is about 60%. These values are considerably higher than the values obtained in the case of the unglazed collector.

The higher efficiency for collectors of this type is reached for periods of time longer than two hours.

The higher values of the thermal power for the high performance flat collector, for the days of August, October, March and May, are situated in the range of 600-800 Wm^{-2}. Even in January it can reach the value of almost 600 Wm^{-2}. These values are higher than in the case of the unglazed collector. In winter, this type of collector is relatively efficient only in the almost clear sky days. In cloudy days of winter this type of collector is equally inefficient, even if it is a high-performance flat collector.

Figs. 12 and 13 present thermal efficiency and thermal power for a low-performance flat collector in different days.

The higher values of thermal efficiency for the low-performance flat collector were 10-15% lower than the similar

ones obtained in the case of the high-performance flat collector. The higher thermal efficiency for this collector type is reached for about only one hour.

In all the considered days, the thermal power on this collector type was lower than in the case of the previously analyzed high-performance flat collector. The maximum value of thermal power for the low-performance flat collector, in August, October and March, is about 600 Wm^{-2}, compared with about 700 Wm^{-2} for the high-performance flat collector. In May, the same values are less than 700 Wm^{-2} compared to almost 800 Wm^{-2}, and in January the two values are about 450 W/m^2 compared to almost 600 Wm^{-2}. In cloudy days of winter this type of collector is equally inefficient.

In the case of the evacuated tubes and of the evacuated tubes with heat pipe collectors, the obtained results were almost in the same range of values. In the case of some manufacturers, the heat pipe construction obtained better results than the evacuated ones, but in the case of other manufacturers the situation was opposite. In these conditions *it was impossible to highlight significant differences between the evacuated and the heat pipe technologies*. Thus, the two types of thermal solar collectors were analyzed together and all those collectors will be indicated as evacuated from this point forward, because the heat pipes are also mounted in evacuated tubes.

Figs. 14 and 15 show thermal efficiency and thermal power for a high-performance evacuated collector on different days.
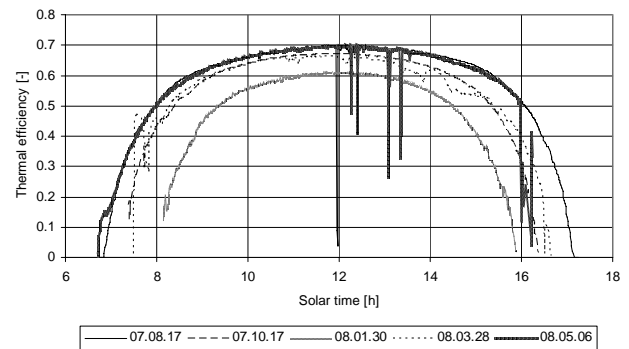

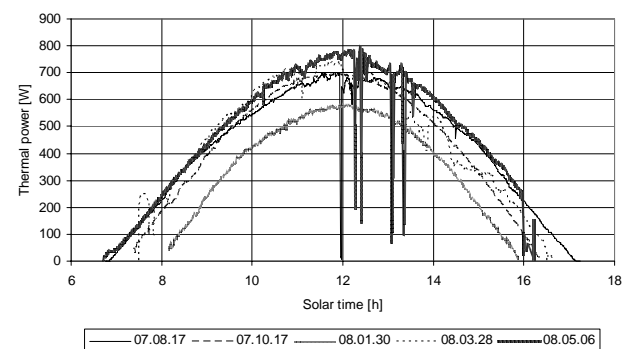Fig. 10. Thermal efficiency for high-performance flat collector – **MT**.

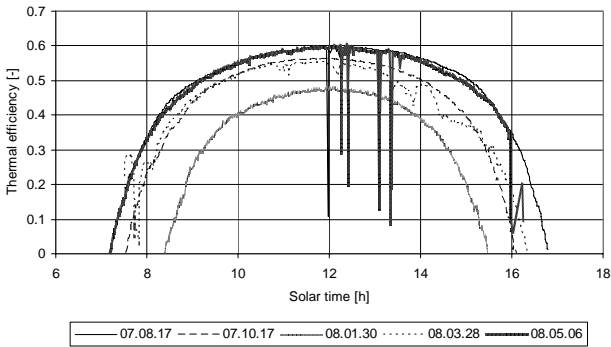Fig. 11. Thermal power for high-performance flat collector – **MT**.

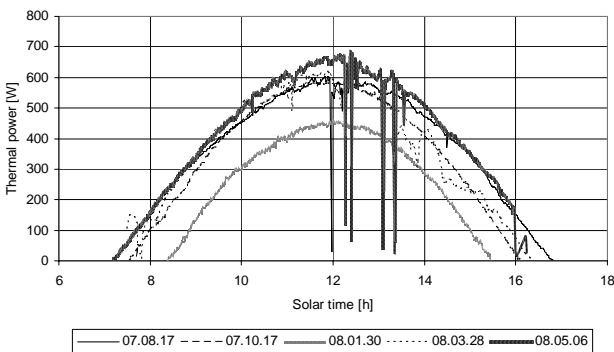Fig. 12. Thermal efficiency for low-performance flat collector – **MT**.

Fig. 13. Thermal power for low-performance flat collector – **MT**.

The higher thermal efficiency values for the high-performance evacuated collectors are about 70-75% during the whole year, less in almost clear sky days. These values are significantly higher than the values obtained in the case of the flat collectors.

It is remarkable that the thermal efficiency of this collector is almost constant for almost eight hours daily in the late summer, autumn and spring and, for more than 4 hours on sunny winter days.

The higher values of thermal power for the high-performance evacuated collector are in all the considered days, in the range of 700-850 Wm^{-2}, values significantly higher than in the case of all types of flat collectors. It is important to mention that with this type of collector, high thermal power can be reached even in cold but with clear sky days of winter.

Figs. 16 and 17 give thermal efficiency and thermal power for a low-performance evacuated collector on different days.

The higher values of thermal efficiency for a low-performance evacuated collector are 20-25% lower than those obtained in the case of high-performance evacuated collectors.

The higher efficiency of this collector type is reached equally for periods of more than four hours daily, in late summer, autumn and spring, or of more than two hours in the sunny days of winter.

The higher values of thermal power for the high performance evacuated collector are in all the considered days, in the range of 400-550 Wm^{-2}. It is important to mention that with this type of collector, higher thermal power does not decrease significantly even in cold, but with clear days of winter.

In order to highlight the behaviour of the different types of thermal solar collectors over longer periods of time, we analyzed the accumulated heat for the previously considered high-performance flat and evacuated collectors. We also considered unglazed collectors.

For longer periods of time we analyzed the decades of previously considered months.

Table 4 presents the values of total accumulated heat in the decades of different months, with different types of solar thermal collectors: evacuated-height performance, flat-height performance and unglazed.

Similar results can be obtained for other particular collectors and for other periods of time: weeks, months, seasons, etc.

Fig. 18 give accumulated heat by three considered collectors.

By analyzing the data from Table 4 and Fig. 18, it can be noticed that in all situations, the unglazed collector's behaviour is dramatically under the ones of the flat and evacuated collector:

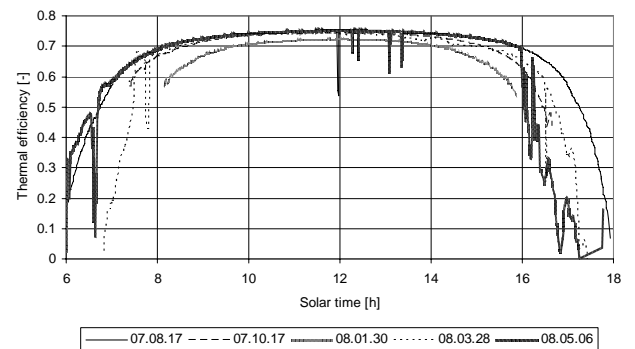• During the nights and low solar radiation days, heat cannot be accumulated in the thermal agent of the col-

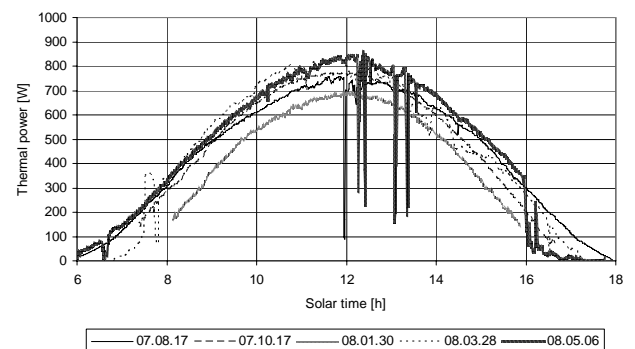Fig. 14. Thermal efficiency for high-performance evacuated collector – **MT**.

Fig. 15. Thermal power for high-performance evacuated collector – **MT**.

Table 4. Values of total accumulated heat in different months with different types of collectors.

Period 10-20 of month	Total accumulated heat for different collector types [MJ]		
	Evacuated height performance	Flat height performance	Unglazed
August 2007	149.06	119.46	44.47
October 2007	122.84	94.09	25.89
January 2008	57.79	33.51	0.29
March 2008	91.52	60.18	14.09
May 2008	168.83	135.32	46.82

lectors, making the curves present horizontal lines. Thus, the collector's behaviour in each day can be easily identified;

- On March 16, 2008 (probably a cloudy day) the efficiency of the unglazed collector was zero for the whole day. The calculated accumulated heat in January 2008 indicated that only in five of the eleven considered days, were values of the thermal efficiency of the unglazed collector higher than zero, but the accumulated heat was insignificant in all that winter period (Table 4);
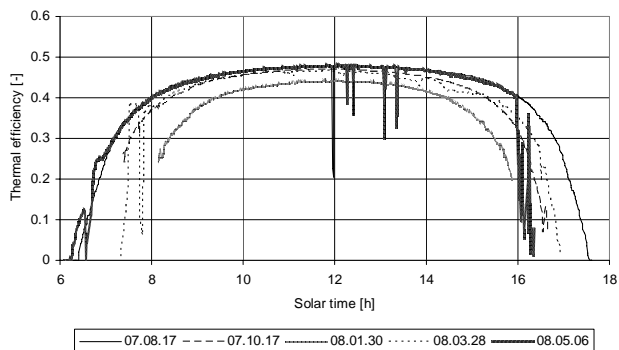- Even in the sunny days of late summer, autumn and spring, the use of unglazed collectors is limited. For

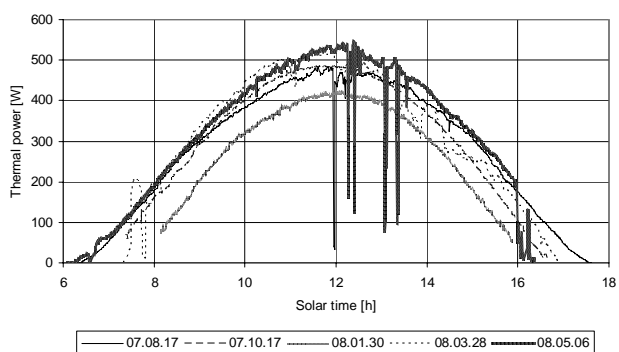Fig. 16. Thermal efficiency for low-performance evacuated collector – **MT**.

Fig. 17. Thermal power for low-performance evacuated collector – **MT.**

technical applications (the best known is swimming pool heating), high surfaces of unglazed collectors are needed, but the price of this technology is equally low and this aspect can explain the use of this type of collector;

- The performances of the flat collectors are normally situated under the ones of the evacuated collectors, but since only the behaviour of high performance collectors of each type were analyzed, in sunny and warm days the low performances of evacuated collectors can become similar to high performance flat collectors. In cold and cloudy days of all seasons, even lower performances of evacuated collectors became better performing than the flat ones;
- In all sunny days the behaviour of all collectors is better performing than on cloudy days.

This study is consistent with similar results previously reported [19]. Based on our measurements, we are able to evaluate the accumulated heat during the whole year. Our paper presents accumulated heat during consecutive ten-day periods for different months (by distinction of [20]), reporting accumulated heat for only several hours.

Summary and Conclusions

Our paper approaches the problem of actuality, concerning the evaluation of solar energy potential. The research is oriented through practical results, presenting equipment performances in the particular conditions of Cluj-Napoca, Romania, and helps in correct selection of thermal solar collectors that are available on the market. Real values of thermal efficiency, thermal power, and accumulated heat are provided for different types of thermal solar collectors in transitory regime, defined by the available measured solar radiation.

A mathematical model to compute the position of the sun on the sky and, equally, the solar radiation on tilted surfaces, representing typical thermal solar collectors was implemented into an original client-server software application then being evaluated and validated.

The accuracy of the implemented mathematical model to compute the position of the Sun on the sky was high-
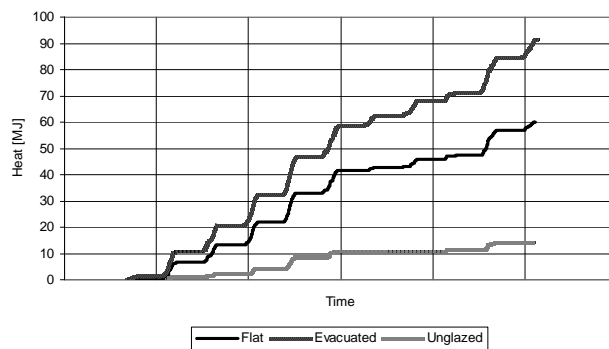

Fig. 18. Accumulated heat for three collectors in March 2008 10-20 – **MT**.

lighted by comparing the obtained results, with known values of astronomical data concerning the sun's position, and by correlating some of the simulation results with the measured solar radiation. Both types of validation tests indicate that the implemented model can be successfully used for the proposed study.

Important results were obtained considering four types of thermal solar collectors, their characteristics being provided by independent testing laboratory or by manufacturers.

Because the solar radiation monitoring system was not conceived to also record ambient temperature, statistical meteorological data were considered, and a sinusoidal variation for this temperature was assumed for the calculations.

Based on the recorded data provided by an original solar radiation monitoring system developed at the Technical University of Cluj-Napoca, Romania, it was possible to approach a complex study of the solar collector's efficiency in transitory working regime.

The important influence of the solar angle of incidence on global solar radiation on the tilted surface of the collectors was highlighted. The paper analyzed only the case of collectors oriented south and tilted 45° from the horizontal plane, but it is in the intention of the authors to also study the complex influence of all the orientation angles of the collectors.

Our paper presents the variation of the solar collector's efficiency and thermal power, obtained in some clear sky days, in different months between August 2007 and May 2008.

It was highlighted that the unglazed and flat collectors are less effective than the evacuated tubes and heat pipe collectors.

Data concerning the variation of the thermal power for each type of the considered collectors was provided. This type of data is important for the behaviour of the thermal solar collectors in transitory regime.

The different behaviour of different types of collectors was also indicated by analyzing the evolution of the heat accumulated into the thermal agent of the collectors, in different periods of consecutive days. This study revealed that better technologies and constructions can provide significantly higher quantities of heat.

An unexpected and important conclusion of the study is that the evacuated tubes and the heat pipe collectors ensure a relatively constant efficiency during almost the whole sunshine duration of the warm and sunny days, characterized by high values of solar radiation. In these days, in the case of high-performance collectors of these types, thermal efficiency remains almost constant, for almost 8 hours in the late summer, autumn and spring and for more than 4 hours even in sunny days of winter. In the case of lower-performances collectors of these types, thermal efficiency remains almost constant for periods of more than 4 hours in late summer, autumn and spring, and for more than 2 hours in the sunny days of winter. In order to evaluate the local solar energy potential in our city, the results presented in the paper will be completed in the next period of time by the solar radiation monitoring system.

The evacuated tubes with cylindrical collector geometry with respect to the sun effectively reduces the incidence angle losses and increases efficiency together with the heat gain. However, the additional cost of investment and maintenance of these collectors may offset the value of the energy collected, reducing global economic efficiency. This element should be taken into consideration for the financial experts' analysis.

The results presented in the paper are obtained by combining in an original way:
*   Data provided by our original solar radiation monitoring system;
*   Data obtained by the simulation of the Sun position on the sky;
*   Data representing technical characteristics of thermal solar collectors, provided by an independent testing laboratory.

Different scientific methods were used to combine the three types of data, to validate the different results that were obtained and to extract the most important conclusions.

All the data and scientific methods were applied for a particular location of the thermal solar collectors, considered the same with the location of the solar monitoring system. The solar collectors were considered to be oriented south and tilted 45° from the horizontal. In these conditions the presented results, obtained in the particular location where solar radiation data were recorded, are of real practical interest.

Nomenclature

Roman Letters

A	Albedo,
F	Computing factor,
I_g	Global radiation on horizontal surface,
I_{gt}	Global radiation on a tilted surface,
I_{grt}	Ground reflected radiation on a tilted surface,
I_{dif}	Diffuse solar radiation on a horizontal surface,
I_{dift}	Diffuse radiation normal on a tilted surface,
I_{difta}	Diffuse radiation normal on a tilted surface (anisotropic assumption),
I_{difti}	Diffuse radiation normal on a tilted surface (isotropic assumption),
I_{dir}	Direct radiation normal on a horizontal surface,
I_{dirt}	Direct radiation normal on a tilted surface,
k_1, k_2	Correction factors,
p	Probability,
P	Thermal power,
Q	Accumulated heat,
r	Pearson correlation coefficient,
y	Day angle.

Greek Letters

α_S	Angle of solar azimuth,
γ_S	Angle of the solar altitude,
δ	Declination of the Sun,

Γ Goodman-Kruskal correlation coefficient,

Δ_t Difference between the temperature of the agent and the ambient temperature,

η Thermal efficiency of solar thermal collectors,

θ Solar angle of incidence on a tilted surface,

η_0 Optical efficiency of solar thermal collectors,

λ Longitude,

ρ Spearman correlation coefficient,

τ_a, τ_b, τ_c Kendall's correlation coefficients,

φ Latitude,

ω Hour angle of the Sun.

Acronyms

EQT: The equation of time,

MLT: Mean local time,

SPF-CH: Solartechnik Prüfung Forschung of Swiss, independent testing laboratory,

ST: Solar time,

TUCN: Technical University of Cluj-Napoca.

References

1.   LERTSATITTHANAKORN C., KHASEE N., ATTHA-JARIYAKUL S., SOPONRONNARIT S., THERDYOTH-IN A., SUZUKI R. O. Performance analysis of a double-pass thermoelectric solar air collector. Solar Energy Materials and Solar Cells, **92**, (9), 1105, **2008**.

2.   KOFFI P. M. E., ANDOH H. Y., GBAHA P., TOURÉ S., ADO G. Theoretical and experimental study of solar water heater with internal exchanger using thermosiphon system. Energy Conversion and Management, **49**, (8), 2279, **2008**.

3.   DUBEY S., TIWARI G. N. Thermal modeling of a combined system of photovoltaic thermal (PV/T) solar water heater. Solar Energy, **82**, (7), 602, **2008**.

4.   ROJAS D., BEERMANN J., KLEIN S. A., REINDL D. T. Thermal performance testing of flat-plate collectors. Solar Energy, **82**, (8), 746, **2008**.

5.   TANIGUCHI M., HIRASAWA S., NAKAUCHI S., TANAKA T. Study of characteristic of evacuated flat plate type solar collector with flow boiling. ASME International Mechanical Engineering Congress and Exposition 2008; Proceedings, **6**, 343, **2008**.

6.   BILGEN E., BAKEKA B. J. D. Solar collector systems to provide hot air in rural applications, Renewable Energy, **33**, (7), 1461, **2008**.

7.   GUEYMARD C. A. Advanced solar irradiance model and procedure for spectral solar heat gain calculation. ASHRAE Transactions, **113**, (1), 149, **2007**.

8.   MZAD H. Prediction of thermal performance of double-glazed solar collector. Archives of Thermodynamics, **29**, (1), 69, **2008**.

9.   GUEYMARD C. A. Interdisciplinary applications of a versatile spectral solar irradiance model: A review. Energy, **30**, (9), 1551, **2005**.

10.   TEPE R., RÖNNELID M., PERERS B. Swedish solar system in combinations with heat pumps. ISES Solar World Congress, Gothenburg, Sweden, June 15-19, **2003**.

11.   JÄNTSCHI L., BĂLAN M., PODAR E., BOLBOACĂ S. D. Thermal Energy Efficiency Analysis for Residential Buildings, IEEE Region 8 Eurocon; Conf. Proc.: 2009-2014. **2007**.

12.   BĂLAN M. C., DAMIAN M., JÄNTSCHI L. Preliminary Results on Design and Implementation of a Solar Radiation Monitoring System. Sensors, **8**, 963, **2008**.

13.   KAPLANIS S., KAPLANIS E. A model to predict expected mean and stochastic hourly global solar radiation I(h;nj) values, Renewable Energy, **8**, 1414, **2007**.

14.   MYERS D. R. Solar radiation modeling and measurements for renewable energy applications: Data and model quality. Energy, **30**, (9), 1517, **2005**.

15.   PEUSER F. A., REMMERS K. H., SCHNAUSS M. Solar Thermal Systems: Successful Planning and Construction. Solarpraxis, Berlin, **2002**.

16.   QUASCHNING V., Understanding Renewable Energy Systems, Earthscan, London **2007**.

17.   LIU B. Y., JORDAN R. C. The Long Term Average Performance of Flat-Plate Solar-Energy Collectors. Solar Energy, **7**, (2), 53, **1963**.

18.   KLUCHER T. M. Evaluation of models to predict insolation on tilted surfaces. National Aeronautics and Space Administration. Lewis Research Center, pp. 1-30, **1978**.

19.   ESBENSEN T. V., KORSGAARD V. Dimensioning of the solar heating system in the zero energy house in Denmark. Solar Energy, **19**, (2), 195, **1977**.

20.   YU Z. T., HU Y. C., HONG R. H., CEN K. F. Investigation and analysis on a cellular heat pipe flat solar heater. Heat and Mass Transfer, **42**, (2), 122, **2005**.

21.   BOLBOACĂ S. D., JÄNTSCHI L. Pearson Versus Spearman, Kendall's Tau Correlation Analysis on Structure-Activity Relationships of Biologic Active Compounds, Leonardo Journal of Sciences **5**, (9), 179, **2006**.